Spillback nozzle characterization using pulsating LED shadowgraphy

Cafaggi, Giovanni; Jensen, Peter Arendt; Clausen, Sønnik; Glarborg, Peter; Dam-Johansen, Kim

Published in:
Experimental Thermal and Fluid Science

Link to article, DOI:
10.1016/j.expthermflusci.2020.110172

Publication date:
2020

Document Version
Peer reviewed version

Spillback nozzle characterization using pulsating LED shadowgraphy

Giovanni Cafaggi[1], Peter Arendt Jensen*[1], Sønnik Clausen[1], Peter Glarborg[1], Kim Dam-Johansen[1]

[1]*Technical University of Denmark, Department of Chemical and Biochemical Engineering, Søltofts Plads, 2800-Kgs.Lyngby, Denmark*

**Corresponding author: paj@kt.dtu.dk*

Abstract

The atomization characteristics of a commercial spillback hydraulic nozzle were investigated in terms of droplet sizes, velocities, trajectories and spray angles. To replicate the fuel spray of a commercial auxiliary marine boiler, an experimental setup was designed and used to atomize water-glycerol solutions with various viscosities. Droplet size, velocity, position and shape were obtained with a novel pulsating LED backlight imaging system that employs a CCD camera to capture pairs of frames with a delay as short as 1µs from one another. The overall spray characteristics of the nozzle and distributions for droplet size and velocity were examined for the operating conditions currently used in the burner and by varying three parameters: pressure drop, flow rate through the nozzle and liquid viscosity. Results include droplet size and velocity distributions in different spray regions, a description of the influence of each varying parameter on global indexes such as the SMD and a comparison with traditional correlations for pressure swirl nozzles.

***Keywords**: atomizer, spray, shadowgraphy, burner, marine*

1 Introduction

Emissions reduction has been a topic of constant interest for industrial processes in the past decades and the marine sector is no exception. The majority of large ships currently use liquid fuels both in the main engine and in the auxiliary systems. To burn any liquid fuel at an effective rate, it is first necessary to convert the liquid stream into fine droplets and mix it with an oxidizer, typically air [1]. A spray nozzle is used to atomize the fuel and the resulting spray properties are determining factors for flame stability and fuel conversion efficiency [2]. The atomization process relation with combustion is complex and has been the subject of numerous studies [3]. The size and velocity of each droplet influence the evaporation rate and thus the position and rate of release of the fuel to the gas phase. In turn, the concentration and mixing of fuel and oxygen in the gas phase will govern the combustion process that provides the heat for the evaporation of the fuel droplets. Understanding the atomization process and spray properties is therefore a key issue in any effort to improve auxiliary marine boilers and reduce their environmental impact. The work presented in this paper is a study aimed at obtaining further insight into spray characteristics in this type of system.

The interactions between atomization and combustion process can be described by Computational Fluid Dynamics models [4]. However, when applying this method to a full-scale system, the spatial discretization needed to observe the first stages of the atomization process is much smaller than the other characteristics lengths [5]. With the recent increase in computational power and developments of DNS, it is possible to

conduct such analysis, but it is still computationally very demanding [2,6–9]. As a simplification, it is possible to inject already atomized droplets in the computational domain, thus avoiding modelling directly the atomization process [10,11]. To do so detailed knowledge of droplet sizes and velocities is needed as an input to the CFD simulation. Several experimental correlations to calculate these data exist for pressure swirl atomizers, but they are usually limited to single parameters such as the Sauter Mean Diameter (SMD), instead of describing the whole size distribution [12]. Moreover, their accuracy is limited by the geometry and operating conditions used in the underlying experiments, and employing different correlations leads to a wide range of results. While the general effects of parameters such as surface tension, viscosity and differential pressure on the spray are generally agreed on, their relative importance varies from source to source. As discussed in the result section, when using the correlations proposed by Lefebvre et al.[13] and Radcliffe et al. [14] on one of the spray characterized in this paper (80 l/h of water, with a ΔP=20 bar), the results vary between 57 and 113 µm for the Sauter Mean Diameter.

Another possibility to obtain these particle size and velocity data is to characterize the spray with experimental methods, thus obtaining information pertaining to the specific nozzle geometry and operating conditions used, here for auxiliary marine boilers [10,15]. This approach also has the benefit of providing a mean of assessing the predictive capabilities of the experimental correlations for the specific nozzle.

The measuring techniques currently available to measure droplet sizes and velocity are several, especially when working in the in the far-field region of a spray [5,16,17]. Few of these techniques also allow measuring both droplet size and velocity simultaneously, thus providing comprehensive information about droplet characteristics [16,18,19]. Possible candidates for such measurements include: Phase Doppler Interferometry (PDI) [17,18], high-resolution imaging [20–24], Interferometric particle imaging [25,26], holography [19,27] and glare point imaging [26]. Among these, high-resolution imaging is relatively simple to implement and, with the recent development in camera sensors and LEDs, the capabilities of this technology have increased drastically [5], making it an ideal candidate for further refinement.

The aim of this paper is to characterize the spray structure produced by a back-spill atomizer in terms of droplet size, velocity and trajectory and to develop and evaluate a novel experimental setup. The spray nozzle is investigated at various supply pressures, liquid viscosities and flow rates in order to reflect possible changes in operating conditions in a full-scale marine auxiliary boiler.

The measurements are made with a novel back-light imaging setup adapted from previous work on solid particle sizing [28]. A technique very similar to the one used has also been proposed for PIV studies under the name of Particle Shadow Velocimetry [29] and provides a solution that lends equally accurate results, with lower equipment costs and that requires significantly less power than traditional PIV measurements.

The optical setup used for this work differs in two ways from conventional shadowgraphy methods for droplet size and velocity measurements. The first is the use of a fast-pulsed single LED as a light source, thus providing short and precise light pulses without using expensive lasers [30–34]. The second is the replacement of high speed cameras [32,35] with a standard CCV camera, decreasing substantially the costs with the only drawback of a longer sampling time.

2 Material and methods

In order to investigate the atomization process, an experimental setup was built at DTU. The setup is composed of two systems: one is the hydraulic and safety devices to reproduce at room temperature the spray generated in the full-scale boiler (Figure 1), the second is a shadowgraphy system to capture the spray and measure the droplet properties (Figure 2).

2.1 The setup

The nozzle used in this study is a commercial spillback hydraulic nozzle, rated for a supply pressure of 20 bar and a maximum flow rate of 125 l/h. The nozzle has a straight orifice with a diameter of 1mm. This is the same nozzle mounted in the Aalborg OS-TCi auxiliary marine boiler, where it is used to atomize different types of fuels including marine diesel and Heavy Fuel Oil (HFO). By regulating the fuel flow rate through the nozzle, it is possible to satisfy a variable steam demand, but for most of the lifetime of the equipment, the atomized flow rate lies in the range between 50 to 112 l/h. Therefore, the spray characterization setup was designed to supply up to 300 l/h, since it uses a single pump that also provides the liquid that is spilled for regulation and through the spillback nozzle. To explore the full range of operation of the nozzle and obtain meaningful data for the actual application, during the experiments the flow rate was kept at 50, 80 and 112 l/h. Another parameter that can be easily changed when operating the boiler is the supply pressure to the nozzle. The nozzle manufacturer gives a design value of 20 bar, but the system can support a relatively broad range of supply pressures without requiring any change. Since this parameter is of fundamental importance for atomization quality in a pressure swirl atomizer [12], the setup has been built with components able to withstand a wide range of pressures and the nozzle has been tested at supply pressures of 15, 20 and 25 bar. The setup is operated with the two backpressure valves, which are used to keep the respective upstream pressure constant, thus regulating supply and spill pressure for the nozzle. A volumetric pump with multiple pistons is used to deliver flow rate in excess of the required amount and part of it is spilled through the first backpressure valve. A membrane tank is used to further reduce any pulsation in the flow. Pressure gauges have been placed as close as possible in the system to the nozzle to monitor supply and spill pressure. The atomized liquid and all the liquid spills are collected into a cylindrical tank and recirculated into the system. To avoid droplet recirculation in the near nozzle region, a raised lid with a hole with the diameter of the boiler burner tube is used and air is sucked by a shielded ventilation connection at the bottom of the tank [36]. The influence of these precautions on the results should be negligible, considering that the spray measurements are taken few centimeters below the nozzle orifice and that the distance to the ventilation and air escape route is approximately one meter. Moreover, it can be argued that this configuration is more similar to that of the full-scale boiler than a closed tank or a completely open environment.

To study the effect of changes in liquid viscosity on the spray characteristics the experiments were repeated with water and water-glycerol solutions [37,38]. This was done to reproduce the viscosities of some of the fuels used in the boiler [39], or achievable with a fuel preheating system [40]. The solutions were designed using the viscosity data found in literature [41]. Due to the higher than normal ambient temperature during the days when the measurements were taken, a slot for a hand held thermocouple has been fitted just after the backpressure valve on the spill line. This made it possible to monitor the liquid temperature throughout the experiments and calculate the actual properties of the liquid during the atomization process. A sample of the solutions has also been collected during the experiments and later analyzed with a Discovery HR2 hybrid rheometer using a Peltier plate to keep liquid at 25°C during the measurement. Values from literature correlations for the viscosity were calculated and lie within the error range of the measurements.

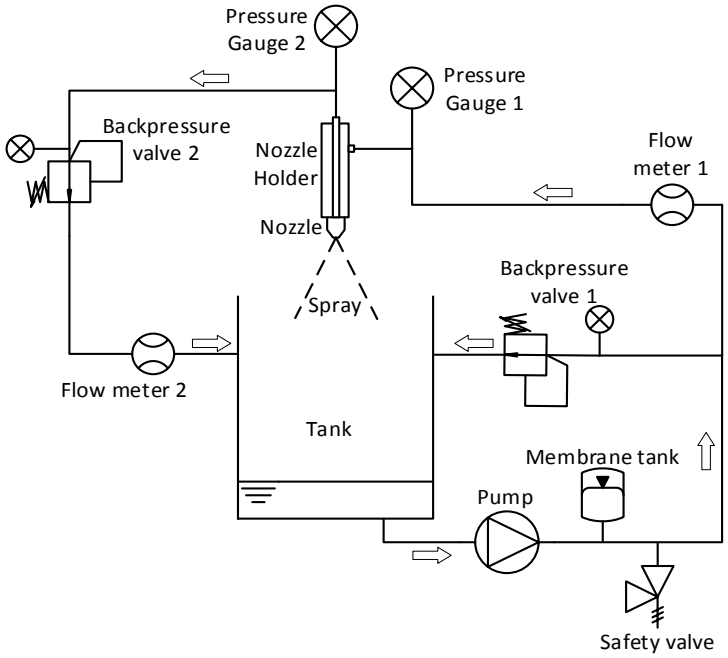

Figure 1: Hydraulic system of the spray characterization setup.

The shadowgraphy setup main components are a CCD camera and an LED pulser, synchronized by a delay generator. This type of system has been described elsewhere [29] and the configuration used in this work has been thoroughly tested in a previous publication [28]. The main characteristic of this setup is that it relies on a fast-pulsed LED instead of a camera shutter to freeze the frames, thus making it possible to obtain consecutive or superimposed images with a delay as low as 1 µs to one another, while avoiding the use of expensive laser illumination systems. Moreover, since the LED can produce light pulses as short as few nanoseconds, the resulting images are "frozen", thus showing the shape of the moving particles with good accuracy and negligible distortion (a particle moving at 50 m/s would move just 1.2µm during a pulse of 24ns). While similar methodologies are employed in recent studies [42], the solution proposed in this paper has been especially developed to replace costly high-speed cameras with a regular CCD camera by synchronizing the shutter and LED signals. The trade-off of this solution is that only pairs of images can be obtained, instead of multiple consecutive frames. While this prevents the tracking of single droplets through more than two consecutive images, it also greatly reduces the costs and droplet size, shape, speed and velocity can still be measured with the same accuracy.

The CCD sensor used is composed of 1296 × 966 pixels for a total size of 4.86 x 3.62 mm, while a telecentric lens provides a magnification of 1.5x. The depth of field of this configuration is 0.86 mm, thus resulting in an observed volume of 6.72 mm^3 and a pixel size of 2.5 x 2.5µm.

To observe different regions of the spray, the system is mounted on a railing system so that the axial and radial distances of the observed volume from the nozzle orifice can be adjusted independently. For this study, all measurements have been taken from 32 to 35 mm downstream of the nozzle orifice and the radial position has been changed in 2.5 mm steps, covering the whole spray cross-section. The number of droplets captured in each frame varies with the position and the spray that is being observed: on the outer fringe of the spray most images are empty, while in the central region more than 50 droplets per image are measured. For each experiment, around 400 image pairs have been recorded at each position. In the periphery of the spray, the

measurements have been stopped when less than 100 droplets were recorded in the corresponding image set. It should of course be noted that this is an arbitrary limit and that statistical significance of the findings is lower in the more dilute regions of the spray.

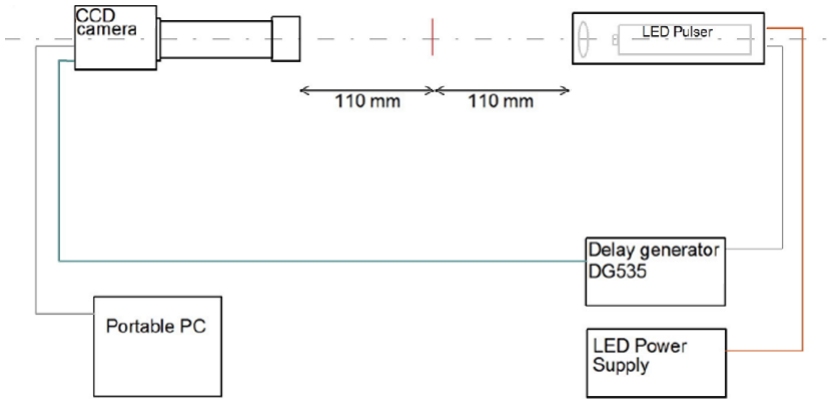

Figure 2: Optical setup diagram.

2.2 Data treatment

To measure the droplet size and velocity accurately, a threshold based droplet recognition method was used together with filtering based on multiple criteria and a simple model to convert the planar measurements to represent the entire cross-section of the spray.

Since fixed parameters are used during these steps, the results are accurate only if the greyscale values of background and droplets are consistent within an image set. Indeed, with shadowgraphy images the background intensity varies due to the light scattering from the out of focus liquid. Thus, images taken in or through a thicker or denser region of the spray will present a lower intensity. Post processing the image sets can help in avoiding this issue. Several image post-processing algorithms have been tested with ImageJ [43], but the one that lent the most consistent results for all image sets was a simple two-step procedure. For each set of images corresponding to a measurement position and operating condition, the average intensity is calculated for each pixel and afterwards, each pixel of each image is divided by the corresponding average value.

From the images obtained, each contiguous dark region is measured if its greyscale value is below a fixed threshold and its boundary gradient above another. The thresholds have been determined based on the greyscale values observed in the images after post-processing, and depend on illumination quality during the experiments. From the areas obtained, the diameter of each droplet is then calculated based on the pixel size and magnification. The delay between the frames is set small enough that the distance each droplet moves between frames is small compared to the distance between droplets, thus each droplet in the first frame is paired with the closest one to its position in the second frame. Since we are interested in single droplets and not gas flow velocity as in classical PIV, the velocity vector of each individual droplet is estimated by measuring the distance of the centre in two consecutive snapshots and dividing it by the delay set between the two frames. Regardless of how sparse the droplets are, it is always possible that some are very close to each other, or that a droplet leaves the sampling volume, and thus different droplets are paired together. To avoid this, it is checked that there is no significant change in droplet shape, sharpness or droplet size between the paired droplets and that the resulting droplet velocity is within reasonable limits. Also, any potential droplet that cannot be matched in the second frame or that has a diameter of less than three pixels is filtered

out, since it is not possible to determine its velocity or shape respectively. This produces a floor value of 7.5µm for the measured droplet diameters (visible in Figure 5b).

To characterize each of the sprays, the railing system was adjusted to move the sampling volume across the spray on a diameter of the circular cross-section of the spray cone. Assuming that the spray is axisymmetric, each sampling volume is representative of all the volume laying at the same distance from the spray axis. To take into account that these volumes are increasingly large the farther away from the spray axis, the contribution of each droplet in all calculations is proportional to its distance from the spray axis. The change that this correction causes is shown in Figure 3, where the cumulative distribution function of droplet size shifts because of the larger fraction of small droplets toward the center of the spray and of bigger ones on the outer region.

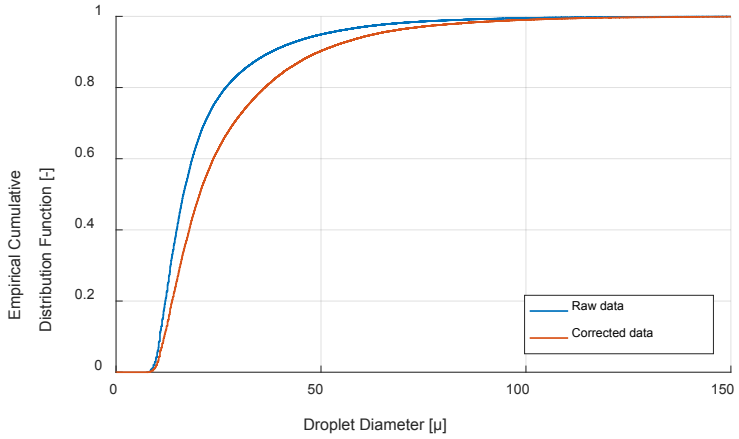

Figure 3: Cumulative Distribution Function of the spray with and without correction for distance from the spray axis of each droplet. Experiment at 80 l/h of water at 25 bars.

2.3 Error evaluation and discussion

The precision of the droplet diameter estimation is determined by several factors. The first is the error on the pixel size, which is calculated with an optical target, and it is subject to an error below 1%. Secondly, there was no adjustment for the depth of field calibration, and while using telecentric optics avoids any distortion of out of focus particles, the effective depth of field for different sized particles could lead to an overestimate of larger droplets. Lastly, there is an error due to the fact that pixels are not infinitesimally small, this leads to an uncertainty on the position of the boundary of each droplet. This error is reduced by processing the images in greyscale, thus also pixels partly obscured are taken into consideration. While it is difficult to give a precise error estimate for each of the contributions, the overall accuracy of the system has been tested in previous work [28] with calibration microspheres. These particles belonged to three different diameter intervals corresponding approximately to 5, 10 and 40 pixels. The measured mean diameter for each of the three groups were within the certified particles size range, which spanned respectively 6.2%, 2.8% and 1.7% of the mean diameter. Therefore, the overall relative measurement error is smaller than these percentages, with the highest uncertainty on the smaller droplets and the lowest on the larger ones.

Another concern when assessing the accuracy of particle or droplet characterization is if the sample size bears statistical significance. This kind of analysis is scarce in the spray characterization literature. A common practice to avoid this issue, is to take a very large sample, speculating that it is sufficient [31,34,44,45]. While

in some works it is possible to find estimates of population size needed for spray characterization, the basis of such claims are generally not given [46,47]. A simple way to gain some insight on this issue is to calculate a relevant parameter for increasingly larger subsets of the droplet population and observe how it converges toward a constant value. While this is a useful indicator, it is very much dependant on the order in which the droplets are considered and on the specific parameter used. To surpass these shortcomings, the procedure was implemented in MatLab code (version R2016a) and repeated for different permutations of the droplet population and for both SMD and average droplet speed (Figure 4a). For each permutation, the number of droplets needed to obtain a relative error on the each parameter smaller than a fixed threshold was found. The number of permutation was increased until a smooth curve was obtained when sorting and plotting the results (10^4 permutations for a population of 10^5 droplets).

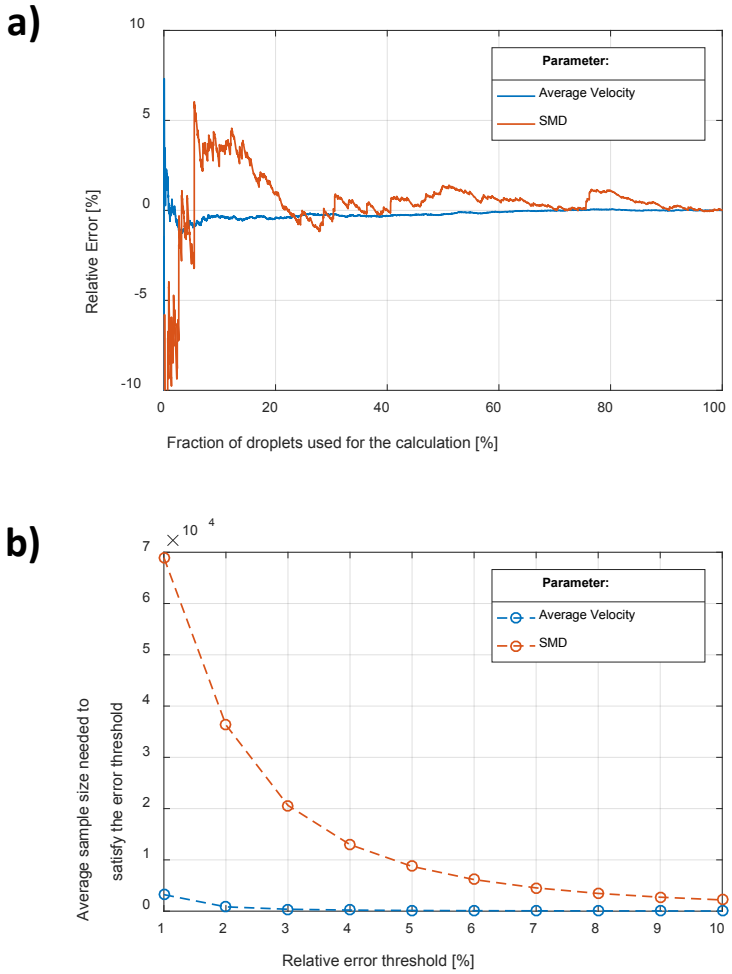

Figure 4: a) Error for the SMD and average velocity for increasingly larger sub-samples of droplets. b) Comparison of average sample size needed to meet different error thresholds for SMD and average velocity. Experiment at 80 l/h of water at 25 bars.

The average sample size needed to meet the error threshold was calculated (Figure 4b) and the process was repeated for thresholds from 1 to 10%. The results of this analysis show that the number of droplets needed to have a reasonably accurate estimate (2 to 4% relative error) of the SMD is between 10^4 and $4x10^4$, while to obtain similar uncertainties on the mean droplet velocity less than a tenth of these amounts are sufficient.

3 Results

The results obtained within this spray characterization study can be divided in two types: detailed information about the droplet size and velocity across the spray, and effects of changes in operating condition on the overall spray characteristics.

3.1 Single droplet measurements across the spray and trends for size fractions

While absolute values and gradients may vary, the same trends have been observed for all measurements for local size, velocity and direction of the droplets across the spray. Therefore, while local measurements have been taken for all experiments, for the sake of simplicity, the plots reported in Figure 5 are for operation with water at 25 bar of supply pressure and a flow rate of 80 l/h, and the average values refer to the image set taken in each position. The plots report both single droplet values, and average values for each sampling position. The average values are given both for the entire population, and droplets above 40 and 80 µm (90th and 98th quantiles respectively for the measurements shown in Figure 5) to visualize different trends dependent on particle size. While the turbulent nature of the flow and its interactions with droplets of different sizes causes the scatter seen in Figure 5, average values still show consistent trends for measurements across the spray and in different experiments. In Figure 5b, it is possible to see that the average droplet size increases farther away from the spray axis, as also reported in other studies [46]. While this was expected, it is interesting to observe that the average size remains constant across the spray when only the larger droplets are considered.

Figure 5c shows that the droplet velocities are on average lower close to the spray axis. In this region, the velocities of the droplets are relatively uniform, with very few droplets moving slower than half of the average value. On the other hand, away from the axis, both the average velocity and the spread increases. By observing the average values found for different droplet size fractions it is also clear that away from the spray axis, larger droplets move faster than smaller ones. While the average velocity increases moving outward, there is also a significant number of droplets with velocities smaller than those found in the hollow core.

In addition to the magnitude of a droplet velocity, to characterize its motion, it is necessary to consider the direction of said motion. When assuming that the tangential component is negligible, it is possible to represent the direction of each droplet in the spray with the angle it forms with the spray axis. The validity of this assumption is supported by the rarity of droplets that move out of focus, compared to that of droplets moving out of the pictures in the image sets. Nonetheless, it is important to remember that in this study as well as in any form of planar measurements, tangential velocities are not measured. The instantaneous direction of the droplet contains important information about their overall trajectory from the orifice to the measuring volume. In Figure 5a, the geometrical angle has been calculated as the angle between the spray axis and the line connecting the nozzle orifice to the sampling position. This quantity is a useful reference since it would be the angle of each droplet if it moved in a straight line from the nozzle orifice to the current position. When comparing these angles to the measured ones, it is evident that they match only at the fringes of the spray and in the center. Looking at the measured angles across the spray, shows that the absolute average value is consistently smaller than the geometric angle, and it presents a complex behavior around the spray axis. When only larger droplets are taken into account, the average angle match the geometric values closely, thus showing that they follow an almost straight trajectory from the nozzle orifice to the

control volume. This suggests that the deviation from the geometrical trajectory is due to the local gas flow field, since inertial and shear forces respectively affect droplets based on their volume and surfaces.

The flow field generated by the entrainment of air into the spray would be consistent with both the observation done for droplet size stratification and deviation from the geometrical trajectory. The air moving toward the hollow core of the spray deviates the droplet trajectories according to their size, thus reducing the angle they form with the spray axis, and increasing the amount of smaller droplets present toward the centre of the spray. This also means that such effects will vary when using the spray nozzle in quiescent or co-flowing air and to study them further gas flow measurements should be conducted.

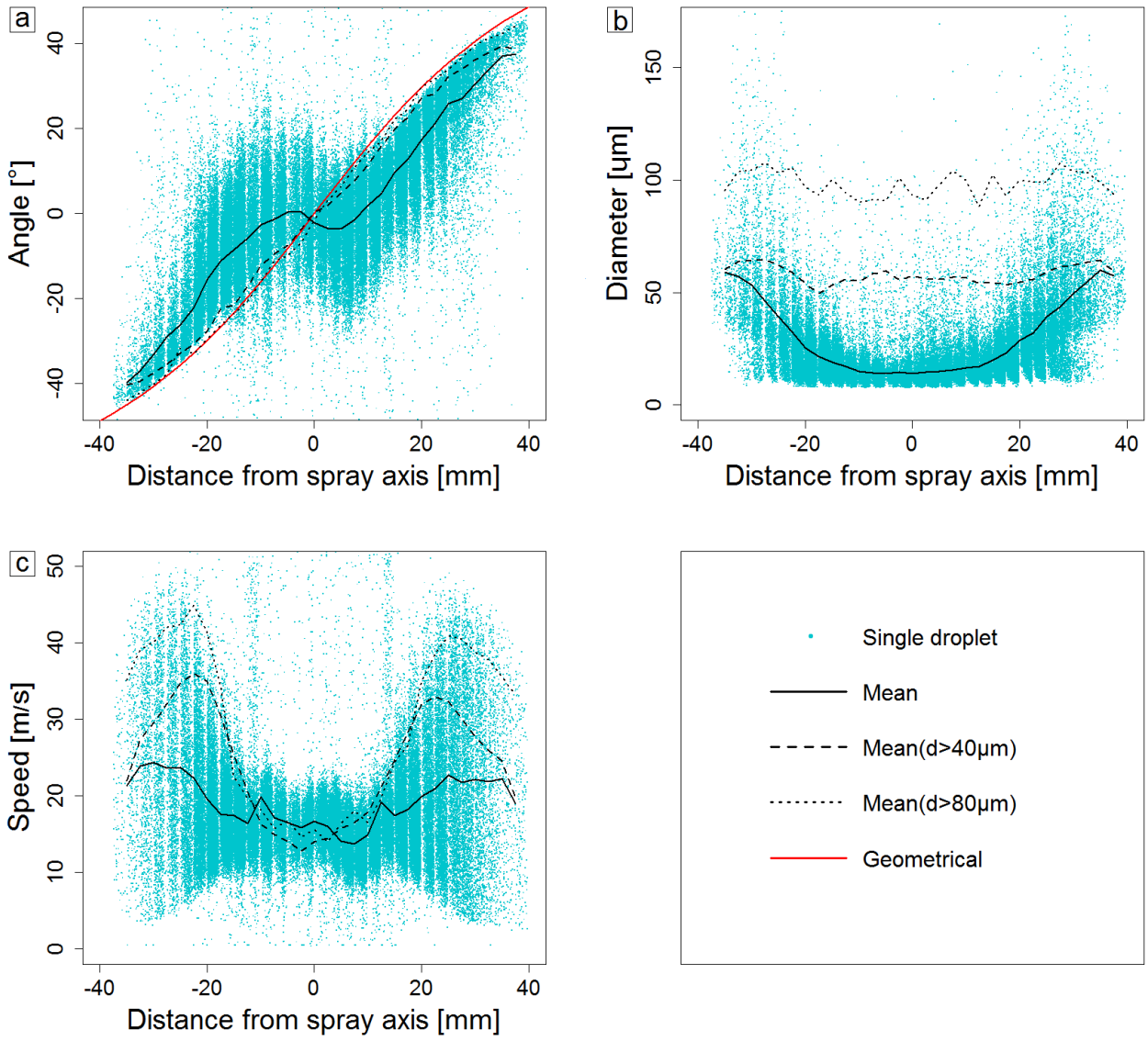

Figure 5: Size (a), velocity (b) and angle (c) across the spray, including averages for different size fractions. The red line represents the geometrical angle formed with spray origin and axis. Experiment at 80 l/h of water at 25 bars.

The vertical stripe pattern of Figure 5 divides droplets of different image sets has two causes. The first is that droplets close to the edge with a non-zero radial velocity might escape the measuring volume before the second image is taken, or might be filtered out from the results if they are partly outside the images, since

they would not comply with the imposed sphericity requirement. The second is that the side of the measuring volume is 86.7 µm smaller than the steps used to move it across the spray, thus leaving a similar gap between the measurements.

3.2 Effects of varying operating conditions on overall spray characteristics

Three main operating conditions of auxiliary marine boilers have a direct influence on the atomization process. The flow rate of the liquid is changed when adjusting to the load of the boiler, the supply pressure to the nozzle can be adjusted with the dedicated pump and the viscosity of the liquid can be reduced with a preheating of the fuel. The experiments with the spray setup included repetitions for different values of each of these parameters to evaluate their impact on the overall spray characteristics. To summarize these results, the SMD, average droplet velocity and spray cone angle have been used.

By adjusting both the backpressure valves (Figure 1) in the spill and supply lines of the nozzle, it was possible to change the supply pressure maintaining the atomized flow constant. Another series of experiments instead was done by maintaining the supply pressure constant and adjusting the spill pressure to obtain three different liquid flow rates through the orifice. In this way, it was possible to observe the contribution of varying supply pressure and flow rate separately. Lastly, the viscosity of the atomized liquid was adjusted by using solutions with different concentrations of water and glycerol and adjusting the setup to obtain the same flow rate and pressures. Overall, the experiments have been carried out using pure water and water-glycerol solutions with viscosities of 1, 3 and 7 cP. The supply pressures have been adjusted to of 15, 20 and 25 bars and the flow rate from 50 to 80 and 112 l/h (Table 1).

Table 1: SMD, average droplet velocity and cone angle for the experimental campaign.

ΔP [bar]	V [l/h]	v [cP]	SMD [µm]	u_{avg} [m/s]	β[°]
20	80	1	57.4	32.1	77
15	80	1	66.4	30.0	72
25	80	1	52.5	33.9	77
20	50	1	53.3	31.0	91
20	112	1	54.1	37.9	66
20	112	3	69.6	39.3	60
20	112	7	77.8	37.6	55

The effect of changing flow rate, supply pressure and viscosity on average droplet velocity and spray cone angle have been investigated. The average droplet velocity shows that an increase in either of the first two parameters results in an increased droplet speed (Table 1). While this result was expected, it was also interesting to observe that for the same relative change, an increase in flow rate produces an effect three times bigger than a change in supply pressure. Viscosity on the other hand does not seem to affect droplet speed significantly. The spray cone angle was defined as the angle between the spray axis, the nozzle orifice and the position of the set of images with the highest liquid fraction for each experiment, and it is therefore on a discrete scale. FromTable 1, it is possible to see how the spray cone angle decreases at higher viscosities and flow rates through the nozzle , while the change in supply pressure has a negligible effect on it (as reported also by [12,33,46]).

Spill-return atomizers are designed to deliver a constant atomization quality with a high turndown ratio. From the results show in Table 1, it is observed that large changes in the flow rate yield almost negligible changes in the SMD (D_{32}).

On the other hand, changes in supply pressure have a clear effect on the droplet size: as in other simplex atomizers [12], higher supply pressure does indeed produce finer droplets. To quantify this effect, the data obtained was compared with experimental correlations found in literature for pressure swirl nozzles, by calculating the proportionality exponent γ as:

$$D_{32} \propto \Delta P^{(\gamma_P)} \tag{1}$$

$$\gamma_P = log_{(\Delta P_a/\Delta P_b)}(D_{32,a}/D_{32,b}) \tag{2}$$

The experiments have been carried out purposely with fixed nozzle geometry, flow rate through the orifice and liquid properties. In these circumstances, several classical experimental correlations for SMD in pressure swirl nozzles can be simplified and written in the same form as equation 1. Moreover, to use the same nomenclature found in literature, pressure difference can be used instead of the supply pressure, since they are equivalent when at constant environment pressure. A value for γ of -0.46 ±0.05 was obtained from the data, matching quite well the values reported in the cited literature, which report values in the range from -0.4 to -0.55 [13,14,48,49].

The same procedure can be applied to the SMD found by changing viscosity of the liquid using water-glycerol solutions. This is done by replacing the pressure difference in equations 1 and 2 with the dynamic viscosity of the liquid. The values obtained for γ in this case is 0.18±0.05, while values between 0.16 and 0.25 are found in literature [13,14,48,49]. While other studies could not find a clear correlation when studying the effects of viscosity [50], the large relative error on this estimate prevents us from confirming or rejecting the literature values. However, a possible explanation for this is that a tendency to entrain air bubbles in the flow was noticed during the experiments and it is suggested that a system without recirculation of the collected liquid should be used in the future.

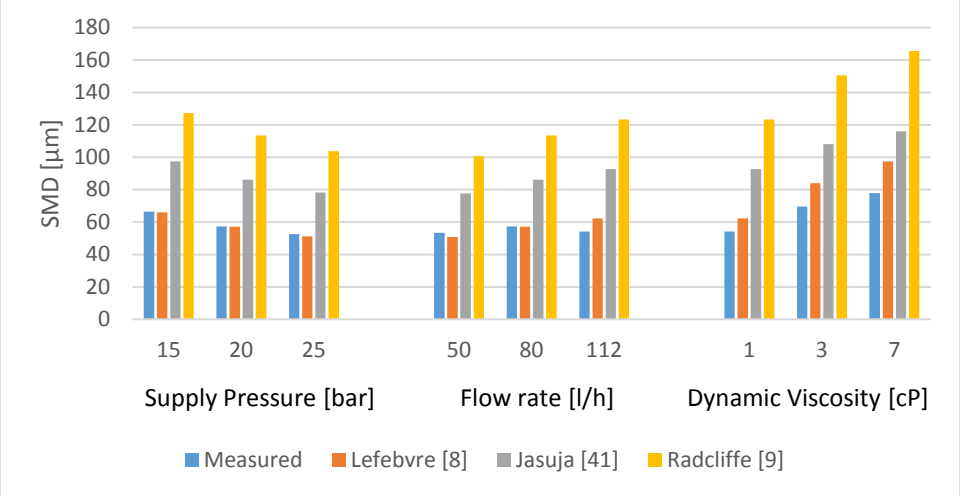

Figure 6: Measured SMD and results for different experimental correlations for the studies operating conditions and sprayed liquids.[13,14,48,49] .

The cited experimental correlations have also been applied to predict the SMD in each experiment and compared with the measured value. From the results of this comparison (Figure 6), it is quite clear that the correlation proposed by Lefebvre et al. [13] leads to the most accurate prediction. While the error found

when changing flow rate or viscosity was up to 25%, the other three correlations tested instead over predicted the SMD by a large margin. Moreover, for the range of tested differential pressures, the prediction match the measurements quite well, with an error below 3%.

Conclusions

The spray generated with an oil burner spill return nozzle has been studied using a LED pulsed shadowgraphy technique. A comprehensive methodology for spray characterization has been developed and presented.

The novel back-light pulsed single LED setup was able to capture pairs of frames with a delay as low as 1 µs and, pixel size of 2.5 µm with an error <1% on the measured spray parameters, proving to be a reliable and economic alternative to systems using lasers and high-speed cameras. Using the presented image post-processing algorithm and a threshold based droplet recognition method it was possible to obtain measurements with an error on the mean particle size ranging from 6.2% to 1.7% depending on the particle size. Overall, the presented configuration of the LED pulsed shadowgraphy technique was demonstrated to have the capability to measure droplet sizes down to 7.5 µm and velocities up to 50 m/s.

Through the statistical analysis of the data thus acquired, it was possible to evaluate the relationship between the population size of the droplet sample and the error on the SMD and the average velocity, showing that a relative error of 2% could have been achieved with $3x10^4$ droplets for the former and 10^3 for the latter. These results both support the validity of the present study, but can also be used as a starting point to assess the sample size needed for future experimental work with similar atomizers.

Seven different operating conditions were investigated by varying the supply pressure to the nozzle (15-20-25 bar), the flow rate (50-80-112 l/h) and the liquid viscosity (1-3-7cP). It was found that a common trend from all experiments was the radial stratification of droplets according to size and velocity, as also shown in other studies [46][51]. The larger droplets of the spray move in a straight line originating from the nozzle orifice and form a hollow cone; on the other hand, the smaller droplets are present also in the core of the cone and deviate significantly from the straight trajectory.

The relation between SMD and changes in supply pressure and viscosity was described with a proportionality exponent γ (Eq.1) and compared to three empirical correlations found in literature [13,14,48]. The γ obtained for supply pressure was -0.46 ±0.05, confirming the literature values. The γ obtained for viscosity was 0.18±0.05, and while it matches the values between 0.16 and 0.25 reported in literature, the large standard deviation suggests that other effects might be in play. The experimental correlation that best approximated our results was the one proposed by Lefebvre et al.[13] and while it could not predict the SMD for changes in flow rate or viscosity, the error for the range of tested differential pressures was less than 3%. The other correlations tested over predicted the SMD by a large margin. Lastly, it was confirmed that changes in atomized flow have little impact on the SMD in back-spill nozzles and that the spray cone angle is increases with decreasing viscosity [30] and flow rate [12].

Acknowledgements

This work was funded by Innovationsfonden, The Danish Maritime Fund and the Technical University of Denmark (DTU) within the Blue INNOship project “Multi Fuel Burners for Low Emissions”. The company Alfa Laval provided the spill back nozzle and valuable information on boiler operation related to the fuel atomization.

Bibliography

[1] A. Williams, Combustion of liquid fuel sprays, Butterworth-Heinemann, 1990. https://doi.org/10.1016/B978-0-408-04113-3.50004-X.

[2] P. Jenny, D. Roekaerts, N. Beishuizen, Modeling of turbulent dilute spray combustion, Prog. Energy Combust. Sci. 38 (2012) 846–887. https://doi.org/10.1016/j.pecs.2012.07.001.

[3] G.M. Faeth, Evaporation and combustion of sprays, Prog. Energy Combust. Sci. 9 (1983) 1–76. https://doi.org/10.1016/0360-1285(83)90005-9.

[4] K. Vogiatzaki, CFD Modeling of Diesel Combustion, in: Encycl. Marit. Offshore Eng., Wiley, 2017. https://doi.org/10.1002/9781118476406.emoe573.

[5] T.D. Fansler, S.E. Parrish, Spray measurement technology: a review, Meas. Sci. Technol. (2015) 1–34. https://doi.org/10.1088/0957-0233/26/1/012002.

[6] Y. Ling, G. Legros, S. Popinet, S. Zaleski, Direct numerical simulation of an atomizing biodiesel jet: Impact of fuel properties on atomization characteristics, in: Proc. 28th Annu. Conf. ILASS-Europe, 2017. https://doi.org/10.4995/ilass2017.2017.5035.

[7] X. Jiang, G. a. Siamas, K. Jagus, T.G. Karayiannis, Physical modelling and advanced simulations of gas-liquid two-phase jet flows in atomization and sprays, Prog. Energy Combust. Sci. 36 (2010) 131–167. https://doi.org/10.1016/j.pecs.2009.09.002.

[8] L. Chen, S.Z. Yong, A.F. Ghoniem, Oxy-fuel combustion of pulverized coal : Characterization , fundamentals , stabilization and CFD modeling, Prog. Energy Combust. Sci. 38 (2012) 156–214. https://doi.org/10.1016/j.pecs.2011.09.003.

[9] A. Déchelette, E. Babinsky, P.E. Sojka, Drop Size Distributions, in: N. Ashgriz (Ed.), Handb. At. Sprays, Springer Science, 2011: pp. 479–495. https://doi.org/10.1007/978-1-4419-7264-4.

[10] J. Park, S. Park, M. Kim, C. Ryu, S. Hyun, Y. Ju, H. Hee, H. Young, CFD analysis of combustion characteristics for fuel switching to bioliquid in oil-fired power plant, Fuel. 159 (2015) 324–333. https://doi.org/10.1016/j.fuel.2015.06.079.

[11] A. Saario, A. Rebola, P.J. Coelho, M. Costa, A. Oksanen, Heavy fuel oil combustion in a cylindrical laboratory furnace: Measurements and modeling, Fuel. 84 (2005) 359–369. https://doi.org/10.1016/j.fuel.2004.10.002.

[12] A.H. Lefebvre, Atomization and Sprays, Hemisphere, Washington, D.C., 1988.

[13] A.H. Lefebvre, Gas Turbine Combustion, Hemisphere, Washington, D.C., 1983.

[14] A. Radcliffe, Fuel Injection, in: High Speed Aerodyn. Jet Propuls., Princeton University Press, Princeton, N.J., 1960.

[15] T. Furuhata, S. Tanno, T. Miura, Y. Ikeda, T. Nakajima, Performance of numerical spray combustion simulation, Energy Convers. Manag. 38 (1997) 1111–1122. https://doi.org/10.1016/S0196-8904(96)00141-0.

[16] C. Tropea, Optical Particle Characterization in Flows, Annu. Rev. Fluid Mech. 43 (2011) 399–426. https://doi.org/10.1146/annurev-fluid-122109-160721.

[17] W.D. Bachalo, Spray diagnostics for the twenty-first century, At. Sprays. 10 (2000) 439–474. https://doi.org/10.1615/AtomizSpr.v10.i3-5.110.

[18] H.-E. Albrecht, M. Borys, N. Damaschke, C. Tropea, Laser Doppler and Phase Doppler Measurement Techniques, Springer, Heidelberg, 2003. https://doi.org/10.1007/978-3-662-05165-8.

[19] J. Burke, C.F. Hess, V. Kebbel, Digital Holography for Instantaneous Spray Diagnostics on a Plane, Part. Part. Syst. Charact. 20 (2003) 183–192. https://doi.org/10.1002/ppsc.200390024.

[20] H.G. Fujimoto, H. Adachi, T. Yano, N. Marubayashi, T. Hori, J. Senda, Spatial Droplets Size Distribution in a Diesel Spray Taken by Photography with Super High Resolution, ILASS - Eur. 2010, 23rd Annu. Conf. Liq. At. Spray Syst. (2010) 1–6.

[21] J.B. Blaisot, J. Yon, Droplet size and morphology characterization for dense sprays by image processing: Application to the Diesel spray, Exp. Fluids. 39 (2005) 977–994. https://doi.org/10.1007/s00348-005-0026-4.
[22] N. Fdida, J.B. Blaisot, Drop size distribution measured by imaging: Determination of the measurement volume by the calibration of the point spread function, Meas. Sci. Technol. 21 (2010). https://doi.org/10.1088/0957-0233/21/2/025501.
[23] C.F. Powell, D. Duke, A.L. Kastengren, Measurements of Diesel Spray Droplet Size with Ultra-Small Angle X-Ray Scattering, in: Proc. 25th Annu. Conf. ILASS-Americas, 2013.
[24] M. Esmail, N. Kawahara, E. Tomita, M. Sumida, Direct microscopic image and measurement of the atomization process of a port fuel injector, Meas. Sci. Technol. 21 (2010). https://doi.org/10.1088/0957-0233/21/7/075403.
[25] N. Fujisawa, A. Hosokawa, S. Tomimatsu, Simultaneous measurement of droplet size and velocity field by an interferometric imaging technique in spray combustion, Meas. Sci. Technol. 14 (2003) 1341–1349. https://doi.org/10.1088/0957-0233/14/8/320.
[26] Y. Zama, M. Kawahashi, H. Hirahara, Simultaneous measurement method of size and 3D velocity components of droplets in a spray field illuminated with a thin laser-light sheet, Meas. Sci. Technol. 16 (2005) 1977–1986. https://doi.org/10.1088/0957-0233/16/10/013.
[27] D.S. Olinger, K.A. Sallam, K. Lin, C.D. Carter, Image Processing Algorithms for Digital Holographic Analysis of Near-Injector Sprays School of Mechanical and Aerospace Engineering Oklahoma State University Stillwater , OK 74078 USA, (2013).
[28] F. Cernuschi, C. Rothleitner, S. Clausen, U. Neuschaefer-rube, J. Illemann, L. Lorenzoni, C. Guardamagna, H. Engelbrecht, Accurate particle speed prediction by improved particle speed measurement and 3-dimensional particle size and shape characterization technique, Powder Technol. 318 (2017) 95–109. https://doi.org/10.1016/j.powtec.2017.05.042.
[29] J. Estevadeordal, L. Goss, PIV with LED: Particle Shadow Velocimetry (PSV) Technique, in: 43rd AIAA Aerosp. Sci. Meet. Exhib., 2012. https://doi.org/10.2514/6.2005-37.
[30] Y. Shenghao, Y. Bifeng, W. Shuai, L. Xifeng, J. Hekun, Y. Jianda, Experimental Investigation on the Early Stage Spray Characteristics with Biodiesel and Diesel, in: Proc. 28th Annu. Conf. ILASS-Europe, Editorial Universitat Politècnica de Valencia, Valencia, Spain, 2017.
[31] M. Kuhnhenn, M.F. Luh, T. V Joensen, I. V Roisman, Experimental Characterization of Spray generated by a Rotary Atomizer Wheel, in: Proc. Proc. 28th Annu. Conf. ILASS-Europe, 2017.
[32] J. Lundberg, Image-Based Characterization of a Medium Velocity Fire Water Nozzle – Preliminary Results, in: D. Bradley, G. Makhviladze, V. Molkov, P. Sunderland, F. Tamanin (Eds.), Seventh Int. Semin. Fire Explos. Hazards, Research Publishing, Providence, RI, USA, 2013. https://doi.org/10.3850/978-981-07-5936-0.
[33] B. Mandal, P. Barman, A. Kushari, Study of Primary Atomization in a Helical Passage Pressure-Swirl Atomizer, in: Proc. 19th Annu. Conf. ILASS-Europe, Nottingham, 2004.
[34] L. Postrioti, G. Brizi, C. Ungaro, M. Mosser, F. Bianconi, A methodology to investigate the behaviour of urea-water sprays in high temperature air flow for SCR de-NOx applications, Fuel. 150 (2015) 548–557. https://doi.org/10.1016/j.fuel.2015.02.067.
[35] S. Minov Vulgarakis, D. Nuyttens, J. Vangeyte, J.G. Pieters, F. Cointault, Spray nozzle characterization using high speed imaging techniques, Precis. Agric. (2013) 569–576. https://doi.org/10.3920/978-90-8686-778-3.
[36] L. Jampolski, A. Sänger, T. Jakobs, G. Guthausen, T. Kolb, N. Willenbacher, Improving the processability of coke water slurries for entrained flow gasification, Fuel. 185 (2016) 102–111. https://doi.org/10.1016/j.fuel.2016.07.102.

[37] Y. Zhan, Y. Kuwata, K. Maruyama, T. Okawa, K. Enoki, M. Aoyagi, T. Takata, Effects of surface tension and viscosity on liquid jet breakup, Exp. Therm. Fluid Sci. 112 (2020) 109953. https://doi.org/10.1016/J.EXPTHERMFLUSCI.2019.109953.
[38] A. Davanlou, J.D. Lee, S. Basu, R. Kumar, Effect of viscosity and surface tension on breakup and coalescence of bicomponent sprays, Chem. Eng. Sci. 131 (2015) 243–255. https://doi.org/10.1016/j.ces.2015.03.057.
[39] L. Zhou, A. Shao, H. Wei, X. Chen, Sensitivity analysis of heavy fuel oil spray and combustion under low-speed marine engine-like conditions, Energies. 10 (2017). https://doi.org/10.3390/en10081223.
[40] J. Bacha, J. Freel, A. Gibbs, L. Gibbs, G. Hemighaus, K. Hoekman, J. Horn, A. Gibbs, M. Ingham, L. Jossens, D. Kohler, D. Lesnini, J. McGeehan, M. Nikanjam, E. Olsen, R. Organ, B. Scott, M. Sztenderowicz, A. Tiedemann, C. Walker, J. Lind, J. Jones, D. Scott, J. Mills, Diesel Fuels Technical Review, Chevron Corp. (2007). https://www.chevron.com/-/media/chevron/operations/documents/diesel-fuel-tech-review.pdf (accessed October 30, 2019).
[41] N. Cheng, Formula for the Viscosity of a Glycerol-Water Mixture, Ind. Eng. Chem. Res. 9 (2008) 3285–3288. https://doi.org/10.1021/ie071349z.
[42] R. Payri, G. Bracho, J. Gimeno, A. Moreno, Investigation of the urea-water solution atomization process in engine exhaust-like conditions, Exp. Therm. Fluid Sci. 108 (2019) 75–84. https://doi.org/10.1016/j.expthermflusci.2019.05.019.
[43] C.A. Schneider, W.S. Rasband, K.W. Eliceiri, NIH Image to ImageJ: 25 years of image analysis, Nat. Methods. 9 (2012) 671–675. https://doi.org/10.1038/nmeth.2089.
[44] D. Cooper, J.J. Chinn, A.J. Yule, Experimental Measurements and Computational Predictions of the Internal Flow Field in a Pressure Swirl Atomizer, in: Proc. 15th Annu. Conf. ILASS-Europe, 1999.
[45] M. Jain, T.K. Kandar, S.F. Vhora, K.N. Iyer, S. V. Prabhu, Experimental investigation of the 700 MWe containment spray system spray nozzles/system, At. Sprays. 27 (2017) 665–690. https://doi.org/10.1615/AtomizSpr.2017019352.
[46] J. Jedelsky, M. Jicha, Energy considerations in spraying process of a spill-return pressure-swirl atomizer, Appl. Energy. 132 (2014) 485–495. https://doi.org/10.1016/j.apenergy.2014.07.042.
[47] A. Tratnig, G. Brenn, Drop size spectra in sprays from pressure-swirl atomizers, Int. J. Multiph. Flow. (2010). https://doi.org/10.1016/j.ijmultiphaseflow.2010.01.008.
[48] A.K. Jasuja, Atomization of Crude and Residual Fuel Oils, ASME J. Eng. Gas Turbines Power. 101 (1979) 250–258.
[49] K.R. Babu, M.V. Narasimhan, K. Narayanaswamy, Prediction of Mean Drop Size of Fuel Sprays from Swirl Spray Atomizers, in: 2nd Int. Conf. Liq. At. Sprays, Madison, Wis., 1982: pp. 99–106.
[50] A. Sänger, T. Jakobs, N. Djordjevic, T. Kolb, Effect of primary instability of a high viscous liquid jet on the spray quality generated by a twin-fluid atomizer, in: Proc. 26th Annu. Conf. ILASS-Europe, ILASS – Europe 2014, Bremen, Germany Effect, 2014.
[51] H. Correia Rodrigues, M.J. Tummers, E.H. van Veen, D.J.E.M. Roekaerts, Effects of coflow temperature and composition on ethanol spray flames in hot-diluted coflow, Int. J. Heat Fluid Flow. 51 (2015) 309–323. https://doi.org/10.1016/j.ijheatfluidflow.2014.10.006.

4 List of Figures

5 Supplementary Material

5.1 Uncertainty sources in the hydraulic system

The sources of errors in the hydraulics of the setup are relative to the accuracy of the measuring the devices present. The flow meters used have a sensitivity of 1.5 l/h and the pressure gauges of 0.5 bars. However, it should be noted that these errors are similar if not smaller to those in the equipment of the full-scale boiler, thus while reducing them could be useful from theoretical understanding of the spray, it would bear no real effect on the application of the results. Another source of error is that the temperature of the system is not controlled and, while the temperature of the liquid has been monitored and considered for all calculations, this account for the average temperature and not for smaller fluctuations.

5.2 Assumption check on sample size analysis

The results obtained in the sample size analysis are consistent with the main assumption needed to carry it out, which is that the sample size on which it is based is large enough to be significant. To further check on this assumption, a sensitivity analysis to assess the influence of the number of droplet measured has been conducted. This analysis showed that the average sample size needed to achieve a certain error is not influenced by the original sample size in the observed range (Figure 7). A more complex behaviour is observed for the SMD, but it is possible to observe that for errors above 2%, the estimate converge for a population around $8x10^4$. This again confirms that the sample used is large enough to draw conclusions above this error threshold.

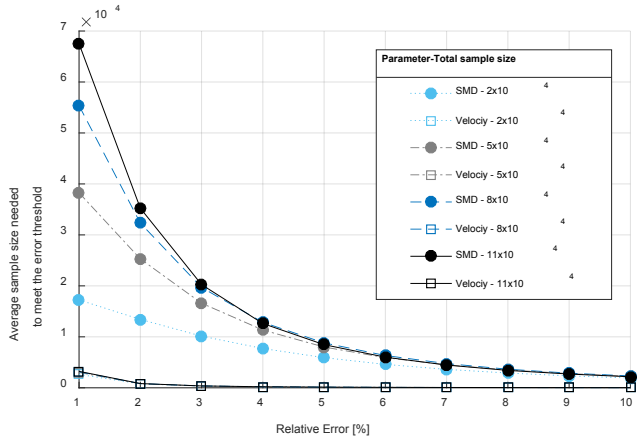

Figure 7: Comparison for different sample size of the number of droplets needed to meet different error thresholds for SMD and average velocity. Experiment at 80 l/h of water at 25 bars.

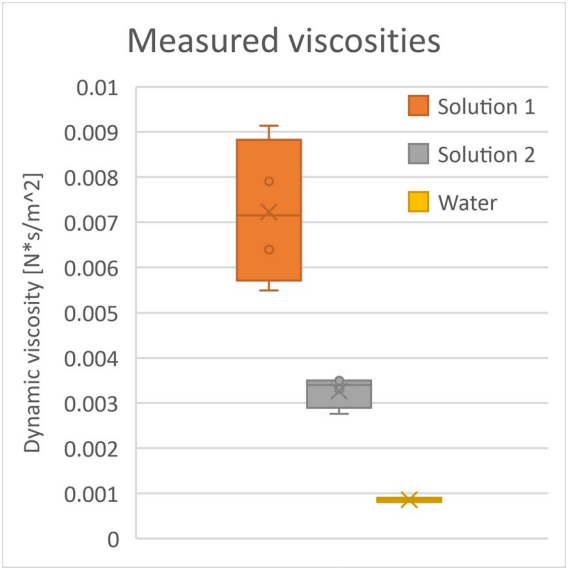

Figure 8: Viscosity measurements of the water/glycerol solution used.